Oecologia (2008) 155:441–454
DOI 10.1007/s00442-007-0932-7

PHYSIOLOGICAL ECOLOGY - REVIEW

Carbon isotopes and water use efficiency: sense and sensitivity

Ulli Seibt · Abazar Rajabi · Howard Griffiths · Joseph A. Berry

Received: 13 July 2007 / Accepted: 28 November 2007 / Published online: 26 January 2008

Abstract We revisit the relationship between plant water use efficiency and carbon isotope signatures ($\delta^{13}C$) of plant material. Based on the definitions of intrinsic, instantaneous and integrated water use efficiency, we discuss the implications for interpreting $\delta^{13}C$ data from leaf to landscape levels, and across diurnal to decadal timescales. Previous studies have often applied a simplified, linear relationship between $\delta^{13}C$, ratios of intercellular to ambient CO_2 mole fraction (C_i/C_a), and water use efficiency. In contrast, photosynthetic ^{13}C discrimination (Δ) is sensitive to the ratio of the chloroplast to ambient CO_2 mole fraction, C_c/C_a (rather than C_i/C_a) and, consequently, to mesophyll conductance. Because mesophyll conductance may differ between species and over time, it is not possible to determine C_c/C_a from the same gas exchange measurements as C_i/C_a. On the other hand, water use efficiency at the leaf level depends on evaporative demand, which does not directly affect Δ. Water use efficiency and Δ can thus vary independently, making it difficult to obtain trends in water use efficiency from $\delta^{13}C$ data. As an alternative approach, we offer a model available at http://carbonisotopes.googlepages.com to explore how water use efficiency and ^{13}C discrimination are related across leaf and canopy scales. The model provides a tool to investigate whether trends in Δ indicate changes in leaf functional traits and/or environmental conditions during leaf growth, and how they are associated with trends in plant water use efficiency. The model can be used, for example, to examine whether trends in $\delta^{13}C$ signatures obtained from tree rings imply changes in tree water use efficiency in response to atmospheric CO_2 increase. This is crucial for predicting how plants may respond to future climate change.

Keywords Carbon isotope discrimination · Evaporative demand · Tree ring analysis · Water use efficiency

Communicated by Russell Monson.

Electronic supplementary material The online version of this article (doi:10.1007/s00442-007-0932-7) contains supplementary material, which is available to authorized users.

U. Seibt · A. Rajabi · H. Griffiths
Department of Plant Sciences, University of Cambridge, Downing Street, Cambridge CB2 3EA, UK

U. Seibt (✉) · J. A. Berry
Department of Global Ecology, Carnegie Institution of Washington, 260 Panama Street, Stanford, CA 94305, USA
e-mail: useibt@globalecology.stanford.edu; useibt@gmail.com

A. Rajabi
Sugar Beet Seed Institute (SBSI), P.O. Box 31585-4114, Karaj, Iran

Introduction

In this paper, we re-examine the relationship between carbon isotope signatures ($\delta^{13}C$) and use of water in plant photosynthesis. As isotopes have become part of the routine analytical procedure, this subject is of considerable interest to researchers across a wide range of scales—whether for the interpretation of molecular physiology, ecological functional groups, regional hydrology or tree ring records. Set against the background of rising atmospheric CO_2, plant $\delta^{13}C$ signals may reflect a range of physiological responses, including stomatal conductance, altered C:N allocation to carboxylation and leaf structure. Our aim is to illustrate the coupling between water use and $\delta^{13}C$ signals based on a robust mechanistic understanding

of their complex relationships. Applying steady-state models of gas exchange, we show how ^{13}C discrimination is related to water use at the leaf level. We then provide an interactive working model, which can be used to examine the sensitivity of plant $\delta^{13}C$ signatures and water use efficiency in a variety of systems.

During the last 150 years, the CO_2 mole fraction in the atmosphere has increased from 280 to 380 μmol mol^{-1}. If rising atmospheric CO_2 levels lead to increased photosynthetic uptake (e.g. Bernacchi et al. 2006) while transpiration rates remain constant or are reduced, the ratio of carbon assimilated to water transpired by plants, i.e. the water use efficiency (WUE), increases. The increase in the atmospheric CO_2 mole fraction thus affects the carbon–water balance of plant gas exchange, the energy balance of forests and the coupled global cycles of carbon and water. Concurrently, the mean $\delta^{13}C$ signature of atmospheric CO_2 ($\delta^{13}C_{atm}$) has decreased from approximately −7 to −8‰ due to fossil fuel combustion and biomass burning of primarily C_3 material (approx. −27‰). To distinguish variations in the $\delta^{13}C$ of source CO_2 from the effects of plant metabolic processes, the $\delta^{13}C$ signatures of plant organic material ($\delta^{13}C_{plant}$) are usually translated to photosynthetic ^{13}C discrimination (Δ; Farquhar and Richards 1984):

$$\Delta = \frac{\delta^{13}C_{atm} - \delta^{13}C_{plant}}{1 + \delta^{13}C_{plant}} \quad (1)$$

Note that permil values such as $\delta^{13}C_{plant}$ need to be divided by 1000 when they occur in terms such as $(1 + \delta^{13}C_{plant})$.

Variations in Δ are frequently used to analyse temporal or spatial trends in plant carbon–water relations. The most often used version of the Farquhar et al. (1982) model—the linear (or reduced) form—relates Δ linearly to C_i/C_a, which is the ratio of intercellular (C_i) to atmospheric (C_a) CO_2 mole fractions:

$$\Delta_{lin} = a + (b' - a)\frac{C_i}{C_a} \quad (2)$$

where a is the fractionation during CO_2 diffusion through the stomata (4.4‰; O'Leary 1981), and b' is the fractionation associated with reactions by Rubisco and PEP carboxylase (27‰; Farquhar and Richards 1984). This equation can implicitly also account for internal CO_2 transfer and is often used to approximate the assimilation weighted C_i/C_a ratio of photosynthesizing leaves:

$$\frac{C_i}{C_a} = \frac{\Delta_{lin} - a}{b' - a} \quad (3)$$

The C_i/C_a ratio reflects the balance between net assimilation (A) and stomatal conductance for CO_2 (g_{sc}) according to Fick's law: $A = g_{sc}(C_a - C_i)$. Stomatal conductances for CO_2 and water vapour (g_{sw}) are related by a constant factor ($g_{sw} = 1.6g_{sc}$), hence linking the leaf gas exchange of carbon and water. The linear relationship between C_i/C_a and Δ (Eq. 2) is often used to calculate the intrinsic water use efficiency, $W_g = A/g_s$, of leaves and plants:

$$W_{g.lin} = \frac{A}{g_{sw}} = \frac{C_a}{1.6}\left(\frac{b' - \Delta_{lin}}{b' - a}\right) \quad (4)$$

The "intrinsic" water use efficiency, i.e. the ratio of net assimilation to stomatal conductance, was introduced to compare photosynthetic properties independent of (or at a common) evaporative demand (Osmond et al. 1980). Thus, W_g derived from plant isotope data is often applied as indicator of long-term trends in the internal regulation of carbon uptake and water loss of plants.

For example, $\delta^{13}C_{plant}$ signatures of tree rings and other plant material have been analysed to investigate the response of plants to increasing atmospheric CO_2 levels. Many studies have reported a relatively larger decrease in $\delta^{13}C_{plant}$ than in $\delta^{13}C_{atm}$, implying a decrease in Δ during the past century (Peñuelas and Azcón-Bieto 1992; Bert et al. 1997; Duquesnay et al. 1998; Arneth et al. 2002; Saurer et al. 2004). For herbarium leaves of Mediterranean trees, a 1‰ decrease in Δ was interpreted as a WUE increase during the past four decades (Peñuelas and Azcón-Bieto 1992). For tree rings of *Abies alba*, decreasing $\delta^{13}C_{plant}$ were interpreted as a 30% WUE increase between 1930 and 1980 (Bert et al. 1997). For conifer species in northern America, decreases in tree ring $\delta^{13}C_{plant}$ over the last century were interpreted as an increase in C_i/C_a with no change in WUE (Marshall and Monserud 1996), or as constant, increasing or decreasing leaf C_i/C_a ratios (Feng 1998). For tree rings of *Fagus sylvatica* formed between 1850 and 1990, a Δ decrease from 18.1 to 16.4‰ was interpreted as a 44% increase in WUE (Duquesnay et al. 1998). For three conifer species at European high-latitude sites, trends in tree ring $\delta^{13}C_{plant}$ were interpreted as a 17–22% increase in WUE (Saurer et al. 2004).

Following the same approach, isotopic analyses of plant material have been applied to compare WUE or C_i/C_a ratios between species or locations. For example, in a comparison of oak species in Western Europe, *Quercus robur* was reported to have a 1‰ larger Δ and, therefore, a 13% lower W_g than *Quercus petraea* (Ponton et al. 2001). Values of $\delta^{13}C_{plant}$ from leaf samples were applied as indicators of assimilation-weighted C_i/C_a ratios, which were then used to evaluate a range of stomatal conductance models for tree gas exchange (Katul et al. 2000).

However, the linear model (Eq. 2) often overestimates Δ (and thus underpredicts W_g), and this deviation increases with assimilation rate (Farquhar et al. 1989). In addition, intrinsic WUE ($W_g = A/g_s$) is not identical to instantaneous WUE ($W_t = A/E$), which is the ratio of assimilation

to transpiration (Farquhar and Richards 1984). This is significant because the interesting parameter from the point of view of the atmosphere, for example in the context of climate change, is integrated WUE, an expression of total carbon gain to total water loss of a leaf, plant or ecosystem, and thus closer related to W_t (via E) than to W_g (via g_s). Here, we discuss the sources and interpretation of $\delta^{13}C_{plant}$ variations in three sections:

(1) We provide a re-analysis of published data, comparing the results of the linear model of Δ (Eq. 2) to those from the classical model (Eq. 6), to make "sense" of the relationships between Δ, C_i/C_a, C_c/C_a and W_g. In particular, we emphasize the role of mesophyll conductance in shaping the expression of Δ in leaf material, and the associated limitations to isotope analyses based on the linear model due to its inherent simplifications.

(2) We discuss the difference between W_g and W_t, in particular the role of evaporative demand. We show how different combinations of trends in plant gas exchange can lead to different trends in W_g and W_t, while these are all consistent with the same trend in Δ (and $W_{g,lin}$; Eq. 4). We also present new data to illustrate that a negative correlation of Δ and W_t at the leaf level may not be passed on to W_p at the whole plant level.

(3) We provide a model to evaluate the "sensitivity" of plant parameters (C_i/C_a, W_g, W_t) and $\delta^{13}C_{plant}$ to changes in environmental conditions and plant properties. This model is available at http://carbonisotopes.googlepages.com. The model calculates gas exchange and $\delta^{13}C_{plant}$ at the leaf level (for comparison with leaf samples), and propagates both gas exchange and isotope values to long-term trends in WUE and $\delta^{13}C_{plant}$ at the canopy scale (for comparison with samples of annual resolution). The model can be used to investigate whether observed trends in Δ indicate changes in the environment, leaf properties, or both, thus providing insight into the physiological mechanisms underlying observed variations in $\delta^{13}C_{plant}$.

Implications of using the linear model of ^{13}C discrimination

Contributions of mesophyll conductance and photorespiration to net ^{13}C discrimination

Internal CO_2 transfer and photorespiration are important components of the isotopic budget of net photosynthesis (Farquhar et al. 1982; Ghashghaie et al. 2003; Wingate et al. 2007) not directly accounted for in the linear model (Eq. 2). When these processes are included (Farquhar et al. 1982), Δ is calculated as:

$$\Delta_c = a\frac{C_a - C_i}{C_a} + a_m\frac{C_i - C_c}{C_a} + b\frac{C_c}{C_a} - f\frac{\Gamma_*}{C_a} \quad (5)$$

where a_m is the fractionation during the internal (mesophyll) CO_2 transfer (1.8‰), b is the fractionation during carboxylation (29‰), f is the fractionation during photorespiration (approx. 8‰), and Γ^* is the CO_2 compensation point in the absence of dark respiration (see Appendix Table 4 for list of parameters). Using Fick's law: $A = g_i(C_i - C_c)$ for the gradient between C_i and C_c, the chloroplast CO_2 mole fraction and mesophyll conductance, g_i, Eq. 5 can be written as:

$$\Delta_c = a + (b - a)\frac{C_i}{C_a} - (b - a_m)\frac{A}{g_i C_a} - f\frac{\Gamma_*}{C_a} \quad (6)$$

The linear (Eq. 2) and classical (Eq. 6) model versions differ by the two terms on the right, corresponding to the offset d introduced by Farquhar et al. (1989), which increases with increasing assimilation rate. Replacing A by the ratio g_s/g_i (see, for example, De Lucia et al. 2003), Eq. 6 can also be written as:

$$\Delta_c = a + \left(b - a + (b - a_m)\frac{g_s}{1.6g_i}\right)\frac{C_i}{C_a} - (b - a_m)\frac{g_s}{1.6g_i} - f\frac{\Gamma_*}{C_a} \quad (6a)$$

For the same Δ from observations (Eq. 1), this relationship yields a different C_i/C_a ratio:

$$\frac{C_i}{C_a} = \frac{\Delta_c - a + (b - a_m)\frac{g_s}{1.6g_i} + f\frac{\Gamma_*}{C_a}}{b - a + (b - a_m)\frac{g_s}{1.6g_i}} \quad (7)$$

as well as a different A/g_s ratio:

$$W_{g,c} = \frac{A}{g_s} = \frac{C_a}{1.6}\left(\frac{b - \Delta_c - f\frac{\Gamma_*}{C_a}}{b - a + (b - a_m)\frac{g_s}{1.6g_i}}\right) \quad (8)$$

Using the classical model, Eqs. 7, 8 show how estimates of C_i/C_a and W_g can be corrected for systematic changes in photorespiration or other factors affecting Δ, which is not possible using Eqs. 3, 4 as these variables are not (or only indirectly) included in the linear model.

Temporal trends inferred from isotope analyses

Several studies have used scenarios of leaf gas exchange regulation to obtain trends in WUE from isotope analysis of plant material [for example, Marshall and Monserud (1996), which includes statistical treatment of trends; Saurer et al. (2004)]. To illustrate the effects of directly including the mesophyll components of the CO_2 pathway

and contributions from photorespiration, we repeated the analysis of $\delta^{13}C_{plant}$ data from tree rings of three conifer species at European high-latitude sites reported by Saurer et al. (2004), chosen because the authors present quantitative examples for three well-defined scenarios. The scenarios (Table 1) represent the regulation of plant gas exchange (here: adjusting g_s) at increased C_a to achieve (1) constant C_i, (2) constant C_i/C_a or (3) constant stomatal drawdown ($C_a - C_i$). Using the linear model (Eqs. 2–4), the scenarios would result in typical trends in Δ and, hence, in $\delta^{13}C_{plant}$ (accounting for the observed 0.83‰ decrease in $\delta^{13}C_{atm}$) and $W_{g,lin}$ (Table 1, top rows). Using the classical model (Eqs. 5–8, all else being equal), the same scenarios would result in somewhat different trends in Δ, $\delta^{13}C_{plant}$ and $W_{g,c}$ (Table 1, bottom rows). Observed changes in $\delta^{13}C_{plant}$ are interpreted by analysing where they fall in the range of changes resulting from the scenarios. Saurer et al. (2004) observed $\delta^{13}C_{plant}$ trends of −0.63, −0.68 and −0.26‰ for three tree species, respectively. In the original analysis, this is closest to the trend expected for constant C_i/C_a, and it is interpreted as increase in W_g by 17.4 ± 4.5, 17.2 ± 2.7 and 22.6 ± 12.1% for the three species, respectively. In the re-analysis with the classical model, the same observed $\delta^{13}C_{plant}$ trends are now intermediate between the C_i and C_i/C_a scenarios. Consequently, the inferred changes in W_g for the same observed $\delta^{13}C_{plant}$ trends increase to 25.0 ± 4.5, 24.2 ± 2.5 and 30.5 ± 12.6%, respectively. The interpretation of the isotope data has changed as the result of directly including mesophyll conductance and photorespiration, even though the g_i value itself remains the same. Furthermore, the analysis is based on the assumption that only C_a and g_s have changed. This is no longer valid if there are concurrent trends in ambient temperature, humidity, light, among others. Additional caveats are discussed below, and the models presented in the last section provide a tool to explore potential implications of changing environmental conditions in the analysis of isotopic trends.

Site and species differences inferred from isotope analyses

The isotope approach has also been applied to investigate species differences in W_g at the same site (e.g. Ponton et al. 2001) and to approximate variables related to plant gas

Table 1 Interpreting observed changes in $\delta^{13}C_{plant}$ based on linear versus classical equations

Change in g_s (%)	g_s	C_a	C_i	C_c	C_i/C_a	$C_a - C_i$	Δ	$W_{g,lin}$	Resulting changes in:		
									Δ	$\delta^{13}C_{plant}$	W_g (%)
Scenarios using Eqs. 2–4 (linear model)											
(1) C_i constant											
	0.055	290	181		0.62	109	18.5	68			
28	0.040	333	181		0.54	152	16.7	95	−1.8	0.95	39
(2) C_i/C_a constant											
	0.055	290	181		0.62	109	18.5	68			
13	0.048	333	208		0.62	125	18.5	78	0.0	−0.83	15
(3) $C_a - C_i$ constant											
	0.055	290	181		0.62	109	18.5	68			
0	0.055	333	224		0.67	109	19.6	68	1.1	−1.93	0
Scenarios using Eqs. (5–8) (classical model)								$W_{g,c}$			
(1) C_i constant											
	0.072	290	203	173	0.70	87	18.5	55			
34	0.048	333	203	173	0.61	130	16.7	82	−1.8	0.99	49
(2) C_i/C_a constant											
	0.072	290	203	173	0.70	87	18.5	55			
13	0.063	333	233	203	0.70	100	19.0	63	0.5	−1.35	14
(3) $C_a - C_i$ constant											
	0.072	290	203	173	0.70	87	18.5	55			
0	0.072	333	246	216	0.74	87	20.0	55	1.5	−2.31	0

See Appendix Table 4 for definition of parameters and units

These scenarios were used by Saurer et al. (2004) to interpret observed changes in $\delta^{13}C_{plant}$ (‰) of tree rings as changes in intrinsic plant water use efficiency (WUE), W_g. Calculations are based on: g_b = 1.5 mol m^{-2} s^{-1}, g_i = 0.2 mol m^{-2} s^{-1}, Γ^* = 30 μmol mol^{-1}

exchange that cannot be measured directly, such as assimilation weighted C_i/C_a ratios for model evaluation (e.g. Katul et al. 2000). However, Δ is determined by C_c/C_a (rather than C_i/C_a), making it sensitive to variations in mesophyll conductance. It is not possible to determine C_c/C_a from the same gas exchange measurements as C_i/C_a because g_i can differ substantially between species and plant functional types (e.g. Vitousek et al. 1990; Lloyd et al. 1992; Griffiths et al. 1999; De Lucia et al. 2003) and with leaf protein content (Lauteri et al 1997), leaf age (Li et al. 2004), nutrient supply (Warren 2004) and other factors. Thus, applying the linear model (Eqs. 2–4) to interpret Δ or $\delta^{13}C_{plant}$ may be problematic. For example, all else being equal, the Δ values of two plants with g_i of 0.2 and 0.4 mol $m^{-2}s^{-1}$ would differ by 1.5‰ (Table 2). Observed Δ gradients of this magnitude often form the basis of physiological interpretations related to plant water use (W_g, C_i/C_a, etc.)—but these plants would have identical W_g values. Additional, smaller effects on Δ may be associated with systematic changes in photorespiration rates due to temperature changes (Table 2), for example when comparing plants along an altitude gradient. The shifts in inferred parameters may be large enough to change the interpretation of observed isotopic differences. For example, Katul et al. (2000) used $\delta^{13}C_{plant}$ of leaf samples to calculate an assimilation weighted C_i/C_a ratio of 0.66 for tree gas exchange and evaluated several stomatal conductance models against this reference ratio. If the value used for b' (Eq. 2) over- or under-estimates the (implicitly included) contribution of g_i, the linear model-derived C_i/C_a ratio may not match the actual mean gas exchange C_i/C_a ratio, which would affect the model comparison and recommendations arising from this study.

Additional processes not included in Eqs. 5–8 are the diffusion of CO_2 through the leaf boundary layer and day respiration (affecting Δ) as well as post-photosynthetic fractionations (affecting $\delta^{13}C_{plant}$). Equations 5–8 can be easily extended to include leaf boundary layer conductance (g_b) in the same way as mesophyll conductance (g_i), but the results are not very sensitive to g_b (see Table 2). However, leaves under field conditions probably have a much lower g_b than those during laboratory measurements in a well-stirred cuvette. The role of day respiration and post-photosynthetic fractionations is difficult to assess because isotope effects associated with the metabolic pathways of carbon in the leaf—and hence the relationships between Δ and the $\delta^{13}C$ signatures of various leaf metabolic compounds—are still largely unknown (Ghashghaie et al. 2001, 2003; Tcherkez et al. 2005; Wingate et al. 2007). Furthermore, the magnitude of fractionation during photorespiration (f) is still under debate (see Gillon and Griffiths 1997), and g_i may vary rapidly, for example in response to changes in C_i (Flexas et al. 2007) or leaf temperature (Warren and Dreyer 2006).

Interpretation of isotopic variations as differences in water use efficiency

Water use efficiency and evaporative demand

The water use efficiency of plants plays an important role in determining the exchange of water between terrestrial ecosystems and the atmosphere and thus affects the global water cycle. It also shapes the water–energy balance of ecosystems. A decrease in water fluxes may mean an

Table 2 Actual and isotope-derived C_i/C_a

	g_b	g_i	C_a	C_s	C_i	C_c	T_{leaf}	Γ^*	actual C_i/C_a	Δ	Back-calculated	
											C_i/C_a	C_i
Mesophyll conductance	1.5	0.1	370	366	260	200	15	30	0.70	17.2	0.56	209
	1.5	0.2	370	366	260	230	15	30	0.70	19.4	0.67	246
	1.5	0.4	370	366	260	245	15	30	0.70	20.6	0.72	265
Leaf temperature	1.5	0.3	370	366	260	240	10	25	0.70	20.3	0.70	261
	1.5	0.3	370	366	260	240	20	36	0.70	20.1	0.69	256
	1.5	0.3	370	366	260	240	30	55	0.70	19.7	0.68	250
Boundary layer conductance	0.9	0.3	370	363	257	237	15	30	0.70	20.0	0.69	255
	1.4	0.3	370	366	260	240	15	30	0.70	20.2	0.70	258
	1.9	0.3	370	367	261	241	15	30	0.70	20.3	0.70	260

See Appendix Table 4 for definition of parameters and units

Actual C_i/C_a was calculated from plant gas exchange and C_i/C_a derived (back-calculated) from isotopes using the linear version of the discrimination equation (Eq. 3). Calculations are based on: $A = 6$ μmol m^{-2} s^{-1}, $g_c = 0.057$ mol m^{-2} s^{-1}

increase in surface temperatures, which is particularly relevant in the context of climate change scenarios. It is therefore both interesting and important to quantify the carbon–water balance of whole plants and ecosystems. At short time scales, the relevant parameter in this context is instantaneous WUE, W_t (=A/E), which is the ratio of assimilation to transpiration (Farquhar and Richards 1984). At longer time scales, respiration and "unproductive" water loss from non-photosynthetic parts of the plant also need to be included (Farquhar et al. 1989). Then, the relevant parameter is integrated WUE, which expresses the ratio of total carbon gain to total water loss of plants or, if soil respiration and evaporation are accounted for, of whole ecosystems. The integrated WUE (W_p) of plants can be written as (Farquhar et al. 1989):

$$W_p = \frac{A}{E}\frac{(1-\phi_c)}{(1+\phi_w)} \quad (9)$$

where ϕ_c is the fraction of assimilated carbon lost in respiration, and ϕ_w is the fraction of total water loss that is "unproductive", i.e. from non-photosynthetic parts of the plant or through open stomata at night. This leads to different sensitivities of intrinsic WUE ($W_g = A/g_s$), instantaneous WUE ($W_t = A/E$), and integrated WUE (W_p), as illustrated in Fig. 1. As a result, W_g inferred from $\delta^{13}C$ data may not be representative for instantaneous W_t or integrated plant WUE (see Cernusak et al. 2007 and references therein). In other words, " ... it is a mistake to associate the Δ value only with water use efficiency, because other water relations parameters are also directly related to the C_i value" (Ehleringer and Cerling 1995).

Most importantly, the rate of transpiration depends on the evaporative demand, i.e. leaf-to-air vapour mole fraction deficit (MFD, or D_a), in addition to stomatal conductance: $E = g_s\ (w_i - w_a)$, where w_a and w_i are vapour mole fractions of ambient air and saturated air at leaf temperature, respectively ($D_a = w_i - w_a$). Thus, intrinsic W_g is related to instantaneous W_t via evaporative demand ($W_t = W_g/D_a$) at the leaf level and to integrated W_p according to (Farquhar and Richards 1984):

$$W_p = \frac{W_g}{D_a}\frac{(1-\phi_c)}{(1+\phi_w)} \quad (10)$$

Changes in W_g, W_t and isotope inferred $W_{g.lin}$ can be uncorrelated (see Fig. 1, Table 3). If g_s and A were kept constant, a decrease in transpiration rate could reflect increasing atmospheric humidity (i.e. decreasing evaporative demand), which would be associated with an increase in W_t but have no effect on W_g. In contrast, if E were to be kept constant because g_s is adjusted to compensate for changes in evaporative demand, W_g would change but not W_t. For Δ, mesophyll conductance has also to be taken into account, which is why changes in $W_{g,lin}$ can be independent from those in either W_g or W_t.

This also means that a range of changes in environmental conditions can lead to the same trend in $\delta^{13}C_{plant}$ (Table 3). For a plausible set of values of air temperature, relative humidity, g_s and A, columns 1 and 2 illustrate the effect of increasing atmospheric CO_2 mole fraction while keeping everything else constant: Δ would increase by 1.5‰ (Eq. 5), $\delta^{13}C_{plant}$ would decrease by 2.3‰ (Eq. 1) and $W_{g,lin}$ would increase by 5% (Eq. 4); however, W_g and W_t would not change—isotope analysis would overestimate the actual change in W_g. Columns 3–6 illustrate how four different scenarios could result in the same $\delta^{13}C_{plant}$ trend (one of the trends observed by Saurer et al. 2004): a decrease in g_s alone (column 3), an increase in temperature and A (column 4), an increase in relative humidity and A, a

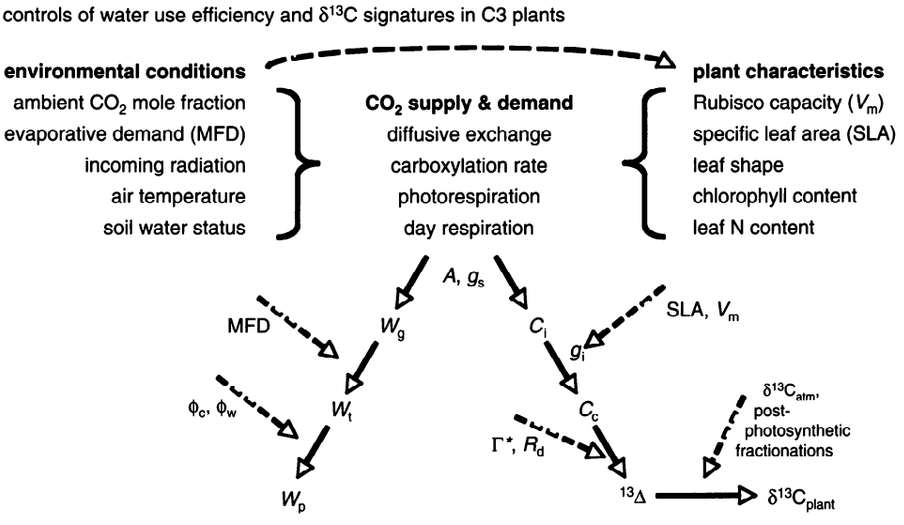

Fig. 1 Factors controlling intrinsic water use efficiency (WUE; $W_g = A/g_s$), instantaneous WUE ($W_t = A/E$), integrated WUE (W_p), net ^{13}C discrimination ($^{13}\Delta$) and $\delta^{13}C$ signatures of plants. The *dashed arrows* indicate independent parameters that need to be considered at each step. This figure is adapted from Griffiths et al. (1999)

Table 3 Different scenarios resulting in the same change in $\delta^{13}C_{plant}$

	Reference	Ca+	gs−	MFD+, A+	MFD−, A+, gs-	MFD−, A+, gs+
T_{air}	15	15	15	17	15	15
h	60	60	60	60	62	70
D_a (MFD)	6.7	6.7	6.7	7.6	6.4	5.0
E	0.73	0.73	0.59	0.83	0.64	0.60
A	6	6	6	7.1	6.7	7.5
Percentage of change			0	18	11	25
g_s	0.11	0.11	0.09	0.11	0.10	0.12
Percentage of change			−20	0	−8	9
C_a	290	333	333	333	333	333
C_i	202	245	223	229	227	231
C_c	172	215	193	193	193	194
C_i/C_a	0.70	0.74	0.67	0.69	0.68	0.69
$C_a - C_i$	88	88	110	104	106	102
Δ	18.5	20.0	18.3	18.3	18.3	18.3
Δ trend		1.5	−0.2	−0.2	−0.2	−0.2
$\delta^{13}C_{atm}$ trend		−0.83	−0.83	−0.83	−0.83	−0.83
$\delta^{13}C_{plant}$ trend		−2.32	−0.63	−0.63	−0.63	−0.63
$W_{g,lin}$	68.3	64.8	80.3	80.3	80.3	80.3
Percentage of change		−5	18	18	18	18
W_g (A/g_s)	55.0	55.0	68.8	65.0	66.5	63.5
Percentage of change		0	25	18	21	15
W_t (A/E)	8.18	8.18	10.22	8.51	10.43	12.59
Percentage of change		0	25	4	27	54

See Appendix Table 4 for definition of parameters and units

Different combinations of changes in environmental conditions and plant gas exchange can result in identical $\delta^{13}C_{plant}$ trends. Calculations are based on: $g_i = 0.2$ mol m^{-2} s^{-1}, $\Gamma^* = 30$ µmol mol^{-1}

decrease in g_s (column 5) or an increase in relative humidity, A and g_s (column 6). Both relative humidity and temperature affect the evaporative demand (MFD, columns 4–6). All scenarios result in the same trends for $W_{g,lin}$ and $\delta^{13}C_{plant}$, but their effects on W_g and W_t are quite different. Even if we derive a good approximation of W_g by using a more detailed analysis (e.g. $W_{g,c}$ from Eq. 8), a comparison of the bottom two rows of Table 3 shows that W_g is not a reliable indicator for W_t if there are no independent estimates of either MFD or E. The model presented in the last section can be used to explore further scenarios. For comparison, model results for the scenarios of Table 3 are presented in an Appendix as Electronic Supplementary Material. In contrast to Table 3, the model takes into account that plant carbon and water fluxes are not independent of each other. These fluxes are computed by the model—they cannot be specified or changed directly, only via adjusting model parameters—which almost always affects more than one variable (see Appendix). Hence, the model output differs slightly from Table 3.

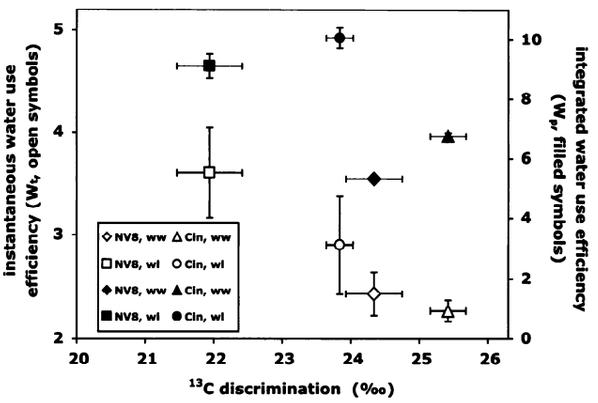

Fig. 2 Instantaneous water use efficiency (W_t, *open symbols*, µmol CO_2 mmol^{-1} H_2O), integrated water use efficiency (W_p; *filled symbols*, g dry matter kg^{-1} H_2O) and ^{13}C discrimination (Δ, ‰) of two sugar beet hybrids, Cinderella (*Cin*) and NV8, grown under well-watered (*ww*) and water-limited (*wl*) conditions (Rajabi 2006). *Error bars* represent SE of measurements ($n = 4$)

Instantaneous and integrated water use efficiency

Measurements of Δ have been used to select C_3 crops with higher W_t at the leaf level, but lower Δ may not always indicate higher W_t or translate into higher W_p at the whole plant level (Condon et al. 2004). As an example, we compare two sugar beet hybrids, NV8 and Cinderella, grown under well-watered and water-limited conditions in controlled experiments (Fig. 2; Rajabi 2006). Gas exchange measurements were used to

determine W_t (μmol CO_2 $mmol^{-1}$ H_2O), Δ was obtained from leaf samples (Eq. 1), and W_p (g dry matter kg^{-1} H_2O) was determined from total dry matter and water use over the season (see Rajabi 2006). Figure 2 illustrates a number of aspects: at the leaf level, Cinderella had higher Δ and lower W_t than NV8 in both treatments, indicating genotypic differences with higher stomatal conductance and/or lower photosynthetic capacity in Cinderella. Under water-limited conditions, both hybrids had higher W_t and lower Δ, consistent with observed lower g_s (data not shown). Water stress can also lead to pronounced decreases in g_i (Monti et al. 2006), which would partly offset the W_t increase associated with lower g_s, but decrease Δ further. The pattern of higher W_p and lower Δ under water stress was preserved for both hybrids at the whole plant level. However, Cinderella had higher Δ as well as higher W_p compared to NV8 at the plant level—the opposite pattern to that found at the leaf level. As a result, Δ was negatively correlated with W_t but not with W_p (Fig. 2). This lack of consistent shifts from leaf to plant level WUE may be related to variations in the "unproductive" respiration and transpiration fractions (φ_c, φ_w, Eq. 9; see Fig. 1). Interactions between plant gas exchange and environmental conditions can lead to complex feedbacks: for example, water stress can affect plant properties, such as photosynthetic capacity, leaf area and thus light interception or transpiration, soil moisture and soil evaporation (see detailed review by Condon et al. 2004).

In Fig. 1, we summarize the way that the environment interacts with leaf traits to determine the $\delta^{13}C$ signature of plant material (Griffiths et al. 1999). At short time scales of hours to days, water use efficiency (W_g, W_t) and isotopic signals (Δ) are both directly controlled by CO_2 supply and demand through photosynthetic rates and stomatal conductance. Thus, variations at these time scales reflect the diurnal cycle of solar radiation, temperature and evaporative demand and synoptic weather patterns. At intermediate time scales of weeks to seasons, they additionally reflect changes in water status associated with soil water uptake (precipitation, root growth, etc.), which can affect short-term controls, such as the regulation of stomatal conductance but also longer-term leaf properties such as mesophyll conductance. Phenological changes such as leaf growth and senescence also contribute to seasonal to interannual patterns. At time scales of decades and longer, large-scale changes in climate or atmospheric circulation as well as ecosystem dynamics (competition, reproductive strategies, nutrient status, etc.) play a role in shaping leaf properties and gas exchange and hence the $\delta^{13}C$ signals and water use of vegetation.

Although affected by similar processes, water use efficiency (W_g, W_t, W_p) and isotopic signals (Δ, $\delta^{13}C_{plant}$) can vary independently because of additional factors that influence them (Fig. 1). Most importantly, W_t depends on evaporative demand in addition to g_s, whereas Δ depends on mesophyll conductance in addition to g_s. If independent estimates of these additional factors are available, W_p can be determined from $\delta^{13}C_{plant}$ via the following series of steps: firstly, $\delta^{13}C_{plant}$ is combined with $\delta^{13}C_{atm}$ to calculate ^{13}C discrimination (Δ, Eq. 1). Secondly, Δ is combined with mesophyll conductance (g_i) to calculate intrinsic WUE (W_g, Eq. 8). Then, W_g is combined with evaporative demand (D_a) to calculate instantaneous WUE ($W_t = W_g/D_a$), the parameter relevant at the leaf level. Finally, if carbon and water losses from non-photosynthetic tissue and the soil are known, W_t and the fractions of these "unproductive" losses can be used to calculate integrated WUE (W_p, Eq. 9), the parameter relevant at the whole plant or ecosystem level. In other words, the path from $\delta^{13}C_{plant}$ to W_p in Fig. 1 traces the arrows on the right (isotopic) side up in the reverse direction and then follows the arrows down on the left (water use) side. In the next section, we present an alternative approach, corresponding to following both left- and right-hand-side arrows down to simultaneously investigate trends in W_t, Δ and $\delta^{13}C_{plant}$.

Sensitivity analysis: potential concurrent trends in W_g, W_t, Δ and $\delta^{13}C_{plant}$

It is important to quantify changes in plant water use efficiency, but it is equally important to determine whether they are caused by adaptations of plant physiological properties to changes in the plant's environment, particularly for predicting how plants may respond to future climate change. In this context, models are best suited to analysing Δ or $\delta^{13}C_{plant}$ data as they can directly account for local or large-scale changes in environmental conditions, such as evaporative demand, or plant properties, such as mesophyll conductance, and their effects on leaf-level W_t and Δ (e.g., Beerling 1994; Le Roux et al. 2001; Arneth et al. 2002; Baldocchi and Bowling 2003). In the following, we present a coupled model that can be used to investigate how trends in W_g, W_t, Δ and $\delta^{13}C_{plant}$ may be affected by such changes.

Leaf level CO_2 uptake represents a balance between the supply of CO_2 limited by diffusional restrictions (g_b, g_s, g_i), and the demand for CO_2 constrained by carboxylation (V_c), oxygenation (photorespiration, V_o) and day respiration (R_d) rates (Farquhar et al. 1980). Net assimilation (A) is computed as the minimum of three potential uptake rates similar to Aranibar et al. (2006). These biochemical rates are functions of leaf properties, such as the catalytic capacity of Rubisco, V_{max}, and environmental conditions,

such as leaf temperature and incoming solar radiation. Stomatal conductance is calculated with the Ball–Berry equation (Ball et al. 1987), which relates g_s to A and the relative humidity (h_s) and CO_2 mole fraction (C_s) at the leaf surface:

$$g_s = m_{BB}\frac{Ah_s}{C_s} + b_{BB} \tag{11}$$

where m_{BB} is the Ball–Berry parameter (dimensionless), and b_{BB} the minimum g_s at $A = 0$. These terms represent the slope and intercept obtained by the linear regression analysis of data from leaf gas exchange studies. Alternatively, the computation of g_s is based on stomatal behaviour with the goal of maximizing daily total carbon gain for a given daily total water use (Cowan and Farquhar 1977). This implies a constant ratio of the sensitivities of E and A to g_s over time: $(\partial E/\partial g_s)/(\partial A/\partial g_s) = \partial E/\partial A = \lambda$, the marginal water cost of carbon gain. At a given temperature, a response of the form of $g_s \propto (w_a - w_i)^{-½}$ keeps $\partial E/\partial A$ approximately constant (Lloyd 1991):

$$g_{sc} = 1.6k\left(\sqrt{\frac{\lambda(C_a - \Gamma)}{1.6(w_a - w_i)}} - 1\right) \tag{12}$$

where k is carboxylation efficiency, and Γ is the CO_2 compensation point. The full classical equation (Farquhar et al. 1982) is used to calculate Δ:

$$\Delta = a_b\frac{C_a - C_s}{C_a} + a\frac{C_s - C_i}{C_a} + a_m\frac{C_i - C_c}{C_a} + b\frac{C_c}{C_a} - f\frac{\Gamma_*}{C_a} - e\frac{R_d}{A + R_d}\frac{C_i - \Gamma_*}{C_a} \tag{13}$$

where a_b is the fractionation during CO_2 diffusion through the leaf boundary layer, and e is the fractionation during day respiration.

The leaf surface variables (leaf temperature, C_s, h_s) are computed from leaf energy balance equations as a function of g_s, g_b and the ambient environment (air temperature, C_a, h_a). There are strong interactions between the components of this coupled system: the photosynthesis model requires C_c and leaf temperature as input variables, which both depend on g_s, while the Ball–Berry model requires A as an input variable. We obtain a simultaneous solution for g_s, A and leaf temperature by numerical methods. For a range of C_c values, two curves for A are calculated, one from the biochemical rates and the other from g_s $[A = g_s(C_a - C_i)]$. A cubic polynomial is then fitted to the difference between the two curves, and the cubic roots of the equation determined analytically, yielding the C_c at which the supply and demand functions are equal. Alternatively, if the lambda version is used, A is computed for two C_c values to determine k from the slope of A versus C_c which is then used to determine g_s (Eq. 12). In both cases, leaf temperature is computed iteratively to close the leaf energy balance.

The canopy profile is approximated by several "big leaf" layers. Each layer receives incoming solar radiation according to a light extinction coefficient. Gas exchange and isotope fractionation are calculated over 1 day (from sinusoidal curves fitted to user defined minima and maxima of temperature and light) to approximate mean environmental conditions during the growing season. As Fig. 3 illustrates, Δ (Eq. 11), W_t (=A/E) and W_g (=A/g_s) are computed from leaf gas exchange in each layer (W_p is not computed, but trends in W_p would correspond closely to those in W_t if the "unproductive" losses (ϕ_c and ϕ_w, Eq. 9) do not vary greatly over time). Equations 4 and 8 are then used to calculate $W_{g,lin}$ and $W_{g,c}$ from Δ so that isotope- and gas exchange-derived W_g values can be compared directly. Corresponding values at the whole-plant level are determined by integrating (A and leaf area weighted) over all layers. This could represent contributions from different canopy layers to cellulose, for example in tree rings (assuming the offset between Δ and $\delta^{13}C$ of cellulose, lignin or other organic compounds is not affected by systematic trends in post-photosynthetic fractionations (Loader et al. 2003)).

Additional "carpet" plots for leaf gas exchange variables (A, E, g_s, C_i/C_a, W_g, W_t, Δ) over the photosynthetic period and along the canopy profile (as in Fig. 3) are presented on the website (address below), illustrating the distinct spatial–temporal patterns of these variables. Integrating these patterns to derive annual trends can thus result in (small but non-linear) shifts in their relationships, in addition to those related to changes in leaf properties and the environment. For example, variations in evaporative demand may lead to inverse diurnal W_g and W_t patterns, with highest W_g but lowest W_t at mid-day, and variations across the canopy profile may be stronger for W_g and Δ than for W_t (see website). At low light and high humidity, W_t and Δ can become largely uncoupled (such as low in forest canopies, or in growth chambers).

A copy of the model is available on the web at http://carbonisotopes.googlepages.com. The site includes a description of how to download and run the model, an example of model output and a list of model input parameters. Users can define constants (such as fractionations and light extinction coefficient) and specify trends over the period of interest. The latter fall in two categories: (1) trends in environmental conditions (w_a, incoming radiation, air temperature) and (2) trends in plant physiological properties (V_{max}, m_{BB}, λ) directly related to plant carbon–water regulation. In addition, users can choose how g_s is calculated (Ball–Berry or λ), whether day respiration (R_d) is light-inhibited and whether mesophyll conductance (g_i) is set to a constant value (Warren and Adams 2006) or

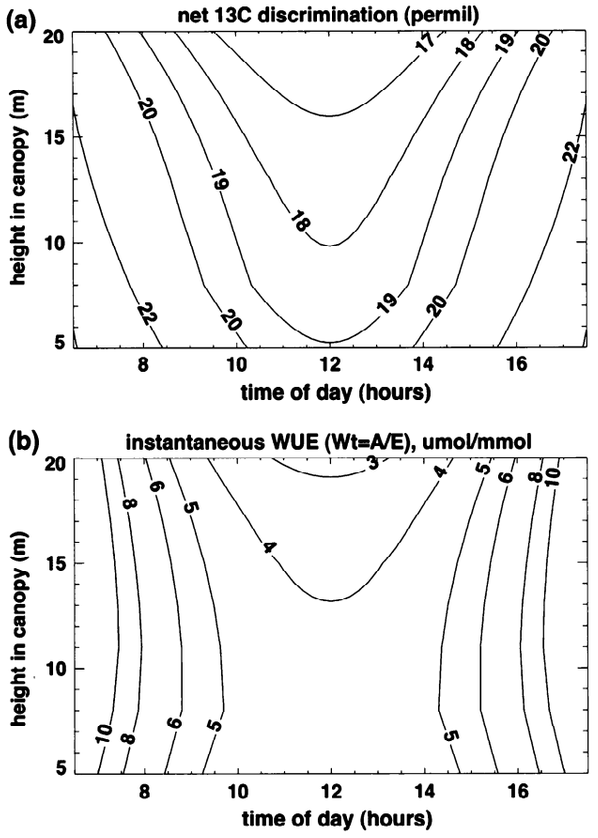

Fig. 3 Model output for ^{13}C discrimination, Δ (**a**) and instantaneous W_t (A/E) (**b**) for leaves across the canopy profile during the photosynthetic period of a day

related to Rubisco content: $g_i = 4{,}800\ V_{max}$ (Aranibar et al. 2006). There are two model versions: (1) for temporal trends ("WanD_trends") and (2) for site or species comparison ("WanD_compare"). The trend version can be used, for example, to examine $\delta^{13}C_{plant}$ time series. For any period between 1850 and 2005, the model computes annual results from user-defined parameters as described above, and the respective C_a and $\delta^{13}C_a$ for each year [see Table 2 in McCarroll and Loader (2004), using data from Robertson et al. (2001) and Francey et al. (1999)]. The comparison version simply computes two sets of results from user-defined parameters.

The model allows a range of scenarios to be explored, in addition to the increase in C_a and associated decrease in $\delta^{13}C_a$. The resulting trends in W_t, W_g, $W_{g,lin}$, $W_{g,c}$ and Δ are expressed relative to the start year of the calculation, so that they can be compared directly. Figure 4 illustrates the model output for two conceptual scenarios: a decrease in V_{max} (Fig. 4a), and an increase in air temperature (Fig. 4b). The relative trend in W_t (approx. 14%; Fig. 4a) is twice as large for the first scenario than for the second (approx. 7%; Fig. 4b). At the same time, both result in comparable relative trends in Δ (approx. 2%) and, hence, also $W_{g,c}$ [Fig. 4a: 15%, Fig. 4b: 14%) and $W_{g,lin}$ (Fig. 4a: 11%, Fig. 4b 12%). However, in one case, shifts in the plant carbon–water balance are due to changing plant physiological properties (Fig. 4a), whereas they are due to changing environmental variables in the other (Fig. 4b), and the latter often leads to diverging trends in W_t versus W_g (Fig. 4).

Based on model results for a variety of scenarios, we observe that: (1) relative trends in W_t, W_g, $W_{g,lin}$ and $W_{g,c}$ often differ from each other, and there is no unique relationship between them, (2) trends in $W_{g,c}$ are closer to those in W_g than trends in $W_{g,lin}$ in most cases and (3) trends can be non-linear due to feedbacks in the coupled system. Observations (or, if these are not available, approximations) of environmental conditions, most importantly evaporative demand, need to be constrained independently to interpret isotope data. This may not apply to tree ring studies that derive and use empirical correlations between $\delta^{13}C_{plant}$ and environmental variables, such as summer air temperature and moisture, but it becomes important when parameters such as C_i/C_a, W_g or W_t are inferred from

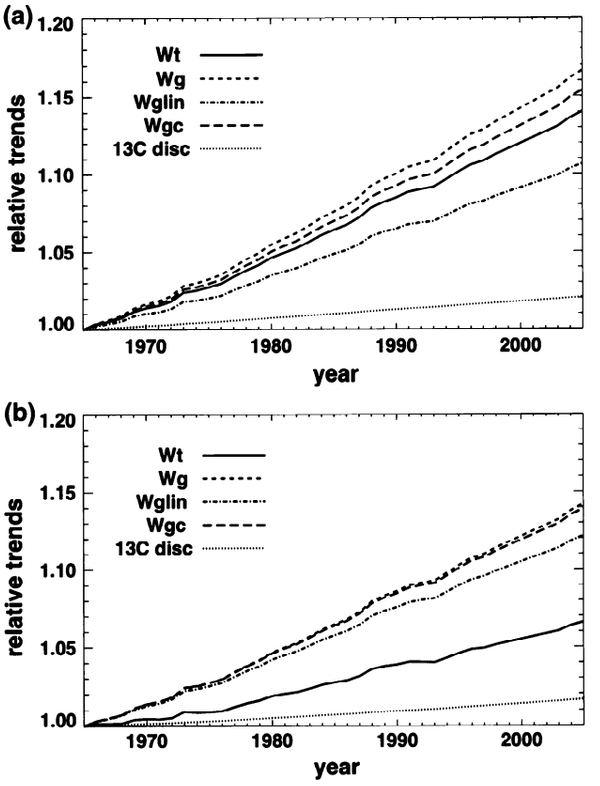

Fig. 4 Model output for relative trends from 1965 to 2005 (relative to first year) resulting from: **a** decrease in V_{max} (40–36 μmol m^{-2} s^{-1}), **b** 3°C increase in air temperature (25–28°C at mid-day). In both scenarios, C_a increases (320–377 μmol mol^{-1}) and $\delta^{13}C_a$ decreases (−7 to −8.1‰); everything else is kept constant

isotope analyses of tree rings and other organic material (see McCarroll and Loader 2004, and references therein).

Summary

A large number of studies have reported systematic changes in plant $\delta^{13}C$ at the landscape scale that contain a wealth of information on the carbon–water balance of plants and ecosystems (for example, Arneth et al. 2002; Hemming et al. 2005). Environmental conditions have short-term effects on $\delta^{13}C_{plant}$: if evaporative demand is altered by atmospheric moisture or temperature, plants usually respond by adjusting g_s, which leads to changes in C_i/C_a (Fig. 1, left column). The environment also has longer term effects on $\delta^{13}C_{plant}$: leaf size and structure may adapt to drought, which can alter mesophyll conductance and thus lead to changes in C_c/C_a (Fig. 1, right column). Environmental gradients at the landscape scale are often coupled, resulting in concurrent trends in temperature, atmospheric humidity, rainfall and soil water availability—for example, across altitude gradients. Furthermore, changes in leaf gas exchange can have complex feedbacks at the leaf to ecosystem scale: g_s determines the partitioning of leaf energy exchange into latent and sensible heat fluxes, affecting both leaf temperature by evaporative cooling and the moisture content of canopy air by transpiration. This means that:

(1) Plant parameters (C_i/C_a, W_g, etc) inferred from $\delta^{13}C$ may be sensitive to processes not directly included in the linear model of Δ (Farquhar et al. 1982). In particular, differences in mesophyll conductance can be large enough to account for the $\delta^{13}C_{plant}$ variations observed in many studies (see Introduction).

(2) Water use efficiency and $\delta^{13}C_{plant}$ can vary independently, reflecting the different factors that influence them (Fig. 1). Most importantly, W_t depends on evaporative demand in addition to g_s, whereas Δ depends on mesophyll conductance in addition to g_s. This is critical for interpreting site and species variations in $\delta^{13}C_{plant}$, but also for long-term trends. Shifts in atmospheric circulation can affect the evaporative demand over a plant's life time or while the plant material (subsequently used for isotope analysis) is assimilated. Thus, $\delta^{13}C_{plant}$ trends alone are not reliable indicators of changes in plant water use efficiency without independent estimates of gas exchange or environmental conditions.

(3) Coupled models of leaf gas exchange (Collatz et al. 1991) provide a more robust, quantitative basis to link plant carbon–water exchange and isotope data to environmental conditions and leaf properties. We offer such a model as an alternative approach to explore the relationships between W_t and Δ and to make use of the extensive data available on $\delta^{13}C_{plant}$ (see above). We expect that our approach will also improve the interpretation of long-term trends in $\delta^{13}C_{plant}$.

Acknowledgements The development of the model was inspired by the ESF/SIBAE Workshop on "Stable Isotopes in Dendroclimatology", GFZ Potsdam, Germany, February 2007. We thank Gerd Helle and the participants of the workshop for discussions. We also thank Eric S. Ober for support. We are grateful to the two reviewers for helpful comments and suggestions. US was funded by a Marie Curie Fellowship of the European Commission (contract MOIF-CT-2004-2704).

Appendix

Table 4 List of variables, parameters and measurement methods (see website for updates: http://carbonisotopes.googlepages.com)

	Parameter	Unit	Measurement method or reference
A	Net rate of assimilation	μmol m^{-2} s^{-1}	In situ measurements (IRGA)
a	Fractionation during diffusion through stomata	4.4‰	Craig (1953)
a_b	Fractionation during boundary layer diffusion	2.9‰	Farquhar (1983)
a_m	Fractionation during internal transfer	1.8‰	
	Sum of fractionation during liquid diffusion	0.7‰	O'Leary (1984),
	Fractionation of CO_2 entering solution	1.1‰	Mook et al. (1974)
b	Mean fractionation during carboxylation by Rubisco and PEP-carboxylase	30‰	Roeske and O'Leary (1984), Guy et al. (1993)
b_{bb}	Ball–Berry minimum stomatal conductance parameter	mol m^{-2} s^{-1}	From leaf level gas exchange data
b'	Mean fractionation during carboxylation and internal CO_2 transfer	27‰	Farquhar and Richards (1984)
C_a	CO_2 mole fraction in ambient air	μmol mol^{-1}	In situ measurements (IRGA)
C_c	CO_2 mole fraction at sites of carboxylation	μmol mol^{-1}	From A, C_i and g_i

Table 4 continued

	Parameter	Unit	Measurement method or reference
C_i	CO_2 mole fraction in intercellular spaces	μmol mol^{-1}	From A, C_s and g_s
C_s	CO_2 mole fraction at leaf surface	μmol mol^{-1}	From A, C_a and g_b
$^{13}\Delta$	Net ^{13}C discrimination during photosynthesis		Equation 1, or in situ measurements (on-line or flasks, e.g. Wingate et al. (2007))
$^{13}\Delta_c$	Net discrimination, classical version		Equation 5 (Eq B24, Farquhar et al. 1982)
$^{13}\Delta_{lin}$	Net discrimination, linear version		Equation 2 (Eq. 11, Farquhar et al. 1982)
$\delta^{13}C_a$	Carbon isotope composition of ambient air	‰	Mass spectrometric analysis
$\delta^{13}C_{plant}$	Carbon isotope composition of plant material	‰	Mass spectrometric analysis
D_a	Vapour mole fraction deficit	mmol mol^{-1}	From w_a and w_i
E	Transpiration rate	mol m^{-2} s^{-1}	In situ measurements (IRGA)
e	Fractionation during decarboxylation	0 to −6‰	Estimate, see Ghashghaie et al. (2001)
f	Fractionation during photorespiration	8‰	Estimate, see Rooney (1988), Gillon and Griffiths (1997)
g_b	Boundary layer conductance to CO_2	mol m^{-2} s^{-1}	From air and leaf temperature data
g_i	Internal (mesophyll) conductance to CO_2	mol m^{-2} s^{-1}	From Δ or fluorescence data (see Evans and von Caemmerer (1996))
g_s	Stomatal conductance to CO_2	mol m^{-2} s^{-1}	Gas exchange measurements (IRGA)
Γ_*	CO_2 compensation point	μmol mol^{-1}	Brooks and Farquhar (1985)
h	Relative humidity	%	From w_a and T_a data
λ	Optimal stomatal conductance parameter ($\partial E/\partial A$)	mol mol^{-1}	From leaf level gas exchange measurements, see Lloyd and Farquer (1994)
m_{bb}	Ball–Berry stomatal conductance parameter		Slope of Eq. 11, from leaf level gas exchange data, see Ball et al. (1987)
p_{atm}	Atmospheric presssure at site	kPa	Sensor data, or nearest met. station
Q	Photosynthetic photon flux density	μmol mol^{-1}	Sensor data, or nearest met. station
R_d	Rate of day respiration	μmol m^{-2} s^{-1}	Extrapolated from nocturnal flux and T_a data (EC tower), or as fraction of A
T_a	Air temperature	°C	Sensor data, or nearest met. station
V_{max}	Maximum carboxylation rate	μmol m^{-2} s^{-1}	From leaf level gas exchange data (A/C_i curves, see Wullschleger (1983))
w_a	Air vapour mole fraction	mmol mol^{-1}	Sensor data, or nearest met. station
w_i	Leaf vapour mole fraction	mmol mol^{-1}	From leaf temperature data (assuming saturated air inside leaf)

References

Aranibar JN, Berry JA, Riley WJ, Pataki DE, Law BE, Ehleringer JR (2006) Combining meteorology, eddy fluxes, isotope measurements, and modeling to understand environmental controls of carbon isotope discrimination at the canopy scale. Glob Chang Biol 12:710–730

Arneth A, Lloyd J, Santruckova H, Bird M, Grigoryev S, Kalaschnikov YN, Gleixner G, Schulze E-D (2002) Response of central Siberian Scots pine to soil water deficit and long-term trends in atmospheric CO_2 concentration. Glob Biogeochem Cycles 16 (1), doi: 10.1029/ 2000GB001374

Baldocchi DD, Bowling DR (2003) Modelling the discrimination of $^{13}CO_2$ above and within a temperate broad-leaved forest canopy on hourly to seasonal time scales. Plant Cell Environ 26:231–244

Ball JT, Woodrow IE, Berry JA (1987) A model predicting stomatal conductance and its contribution to the control of photosynthesis under different environmental conditions. In: Biggins I (ed) Progress in Photosynthesis Research, vol. IV. Proc Int Congr Photosynthesis. Martinus Nihjoff, Dordrecht, pp 221–224

Beerling DJ (1994) Predicting leaf gas exchange and $\delta^{13}C$ responses to the past 30,000 years of global environmental change. New Phytol 128:425–433

Bernacchi CJ, Leakey ADB, Heady LE, Morgan PB, Dohleman FG, McGrath JM, Gillespie KM, Wittig VE, Rogers A, Long SP, Ort DR (2006) Hourly and seasonal variation in photosynthesis and stomatal conductance of soybean grown at future CO_2 and ozone concentrations for 3 years under fully open-air field conditions. Plant Cell Environ 29:2077–2090

Bert D, Leavitt SW, Dupouey JL (1997) Variations of wood $\delta^{13}C$ and Water-use efficiency of *Abies alba* during the last century. Ecology 87:1588–1596

Brooks A, Farquhar GD (1985) Effect of temperature on the CO_2/O_2 specificity of ribulose 1,5-bisphosphate carboxylase oxygenase and the rate of respiration in the light: estimates from gas exchange measurements on spinach. Planta 165:397–406

Cernusak LA, Aranda J, Marshall JD, Winter K (2007) Large variation in whole-plant water-use efficiency among tropical tree species. New Phytol 173:294–305

Collatz GJ, Ball JT, Grivet C, Berry JA (1991) Physiological and environmental regulation of stomatal conductance, photosynthesis

and transpiration: a model that includes a laminar boundary layer. Agric For Meteorol 54:107–136
Condon AG, Richards RA, Rebetzke GJ, Farquhar GD (2004) Breeding for high water-use efficiency. J Exp Bot 55:2447–2460
Cowan IR, Farquhar GD (1977) Stomatal function in relation to leaf metabolism and environment. Symp Soci Exp Biol 31:471–505
Craig H (1953) The geochemistry of the stable carbon isotopes. Geochim Cosmochim Acta 3:53–92
De Lucia EH, Whitehead D, Clearwater MJ (2003) The relative limitation of photosynthesis by mesophyll conductance in co-occurring species in a temperate rainforest dominated by the conifer *Dacrydium cupressinum*. Funct Plant Biol 30:1197–1204
Duquesnay A, Breda N, Stievenard M, Dupouey JL (1998) Changes of tree-ring $\delta^{13}C$ and water-use efficiency of beech (*Fagus sylvatica* L.) in north-eastern France during the past century. Plant Cell Environ 21:565–572
Ehleringer JR, Cerling TE (1995) Atmospheric CO_2 and the ratio of intercellular to ambient CO_2 concentrations in plants. Tree Physiol 15:105–111
Evans JR, von Caemmerer S (1996) Carbon dioxide diffusion inside leaves. Plant Physiol 110:339–346
Farquhar GD (1983) On the nature of carbon isotope discrimination in C4 species. Aust J Plant Physiol 10:205–226
Farquhar GD, Richards RA (1984) Isotopic composition of plant carbon correlates with water use efficiency of wheat genotypes. Aust J Plant Physiol 11:539–552
Farquhar GD, Caemmerer von S, Berry JA (1980) A biochemical model of photosynthetic $C0_2$assimilation in leaves of C_3 species. Planta 149:78–90
Farquhar GD, O'Leary MH, Berry JA (1982) On the relationship between carbon isotope discrimination and the intercellular carbon dioxide concentration in leaves. Aust J Plant Physiol 9:121–137
Farquhar GD, Ehleringer JR, Hubick KT (1989) Carbon isotope discrimination and photosynthesis. Ann Rev Plant Physiol Plant Mol Biol 40:503–537
Feng X (1998) Long-term c_i/c_a response of trees in western North America to atmospheric CO_2 concentration derived from carbon isotope chronologies. Oecologia 117:19–25
Flexas J, Diaz-Espejo A, Galmés J, Kaldenhoff R, Medrano H, Ribas-Carbo M (2007) Rapid variations of mesophyll conductance in response to changes in CO_2 concentration around leaves. Plant Cell Environ 30:1284–1298
Francey RJ, Allison CE, Etheridge DM, Trudinger CM, Enting IG, Leuenberger M, Langenfelds RL, Michel E, Steele LP (1999) A 1,000-year high precision record of $\delta^{13}C$ in atmospheric CO_2. Tellus 51B:170–193
Ghashghaie J, Duranceau M, Badeck F-W, Cornic G, Adeline M-T, Deleens E (2001) $\delta^{13}C$ of CO_2 respired in the dark in relation to $\delta^{13}C$ of leaf metabolites: comparison between *Nicotiana sylvestris* and *Helianthus annuus* under drought. Plant Cell Environ 24:505–515
Ghashghaie J, Badeck F, Lanigan G, Nogues S, Tcherkez G, Deleens E, Cornic G, Griffiths H (2003) Carbon isotope fractionation during dark respiration and photorespiration. Phytochem Rev 2:145–162
Gillon JS, Griffiths H (1997) The influence of (photo) respiration on carbon isotope discrimination in plants. Plant Cell Environ 20:1217–1230
Griffiths H, Borland AM, Gillon JS, Harwood KG, Maxwell K, Wilson JM (1999) Stable isotopes reveal exchanges between soil, plants and the atmosphere. In: Press MC, Scholes JD, Barker MG (eds) Advances in physiological plant ecology. Blackwell Science, Oxford, pp 415–441
Guy RD, Fogel ML, Berry JA (1993) Photosynthetic fractionation of the stable isotopes of oxygen and carbon. Plant Physiol 101:37–47
Hemming D, Yakir D, Ambus P, 31 co-authors (2005) Pan-European $\delta^{13}C$ values of air and organic matter from forest ecosystems. Glob Chang Biol 11:1065–1093
Katul GG, Ellsworth DS, Lai C-T (2000) Modelling assimilation and intercellular CO_2 from measured conductance: a synthesis of approaches. Plant Cell Environ 23:1313–1328
Lauteri M, Scartazza A, Guido MC, Brugnoli E (1997) Genetic variation in photosynthetic capacity, carbon isotope discrimination and mesophyll conductance in provenances of *Castanea sativa* adapted to different environments. Funct Ecol 11:675–683
Le Roux X, Bariac T, Sinoquet H, Genty B, Piel C, Mariotti A, Girardin C, Richard P (2001) Spatial distribution of leaf water-use efficiency and carbon isotope discrimination within an isolated tree crown. Plant Cell Environ 24:1021–1032
Li C, Liu S, Berninger F (2004) *Picea* seedlings show apparent acclimation to drought with increasing altitude in the eastern Himalaya. Trees 18:277–283
Lloyd J (1991) Modelling stomatal responses to environment in *Macadamia integrifolia*. Aust J Plant Physiol 18:649–660
Lloyd J, Farquhar GD (1994) ^{13}C discrimination during CO_2 assimilation by the terrestrial biosphere. Oecologia 99:201–215
Lloyd J, Syvertsen JP, Kriedemann PE, Farquhar GD (1992) Low conductances for CO_2 diffusion from stomata to the sites of carboxylation in leaves of woody species. Plant Cell Environ 15:873–899
Loader NJ, Robertson I, McCarroll D (2003) Comparison of stable carbon isotope ratios in the whole wood, cellulose and lignin of oak tree-rings. Palaeogeogr Palaeoclimatol Palaeoecol 196:395–407
Marshall JD, Monserud RA (1996) Homeostatic gas exchange parameters inferred from $^{13}C/^{12}C$ in tree rings of conifers. Oecologia 105:13–21
McCarroll D, Loader NJ (2004) Stable isotopes in tree rings. Q Sci Rev 23:771–801
Monti A, Brugnoli E, Scartazza A, Amaducci MT (2006) The effect of transient and continuous drought on yield, photosynthesis and carbon isotope discrimination in sugar beet (*Beta vulgaris* L.). J Exp Bot 57:1253–1262
Mook WG, Bommerson JC, Staverman WH (1974) Carbon isotope fractionations between dissolved bicarbonate and gaseous carbon dioxide. Earth Planet Sci Lett 22:169–176
O'Leary MH (1981) Carbon isotope fractionation in plants. Phytochemistry 20:553–567
O'Leary MH (1984) Measurement of the isotopic fractionation associated with diffusion of carbon dioxide in aqueous solution. J Phys Chem 88:823–825
Osmond CB, Björkman O, Anderson DJ (1980) Physiological processes in plant ecology. Springer, New York
Peñuelas J, Azcón-Bieto J (1992) Changes in leaf $\Delta^{13}C$ of herbarium plant species during the last 3 centuries of CO_2 increase. Plant Cell Environ 15:485–489
Ponton S, Dupouey J-L, Breda N, Feuillat F, Bodenes C, Dreyer E (2001) Carbon isotope discrimination and wood anatomy variations in mixed stands of *Quercus robur* and *Quercus petraea*. Plant Cell Environ 24:861–868
Rajabi A (2006) Carbon isotope discrimination and selective breeding of sugar beet (*Beta vulgaris* L.) for drought tolerance. PhD thesis, University of Cambridge, UK
Robertson A, Overpeck J, Rind D, Mosley-Thompson E, Zielinski G, Lean J, Koch D, Penner J, Tegen I, Healy R (2001) Hypothesized climate forcing time series for the last 500 years. J Geophys Res 106:14783–14803
Roeske CA, O'Leary MH (1984) Carbon isotope effects on the enzyme-catalyzed carboxylation of ribulose bisphosphate. Biochemistry 23:6275–6284

Rooney MA (1988) Short-term carbon isotope fractionation by plants. PhD thesis, University of Wisconsin, Madison

Saurer M, Siegwolf RTW, Schweingruber FH (2004) Carbon isotope discrimination indicates improving water-use efficiency of trees in northern Eurasia over the last 100 years. Glob Chang Biol 10:2109–2120

Tcherkez G, Cornic G, Bligny R, Gout E, Ghashghaie J (2005) In vivo respiratory metabolism of illuminated leaves. Plant Physiol 138:1596–1606

Vitousek PM, Field CB, Matson PA (1990) Variation in foliar $\delta^{13}C$ in Hawaiian *Meterosideros polymorpha*: a case of internal resistance? Oecologia 84:362–370

Warren CR (2004) The photosynthetic limitation posed by internal conductance to CO_2 movement is increased by nutrient supply. J Exp Bot 55:2313–2321

Warren CR, Adams MA (2006) Internal conductance does not scale with photosynthetic capacity: implications for carbon isotope discrimination and the economics of water and nitrogen use in photosynthesis. Plant Cell Environ 29:192–201

Warren CR, Dreyer E (2006) Temperature response of photosynthesis and internal conductance to CO_2: results from two independent approaches. J Exp Bot 57:3057–3067

Wingate L, Seibt U, Moncrieff JB, Jarvis PG, Lloyd JJ (2007) Variations in ^{13}C discrimination during CO_2 exchange by *Picea sitchensis* branches in the field. Plant Cell Environ 30:600–616

Wullschleger SD (1983) Biochemical limitations to carbon assimilation in C_3 plants—a retrospective analysis of the A/C_i curves from 109 species. J Exp Bot 44:907–920